J Mater Sci: Mater Med
DOI 10.1007/s10856-011-4506-1

Novel biodegradable, biomimetic and functionalised polymer scaffolds to prevent expansion of post-infarct left ventricular remodelling

Caterina Cristallini · Mariacristina Gagliardi · Niccoletta Barbani · Daniela Giannessi · Giulio D. Guerra

Received: 30 July 2011 / Accepted: 16 November 2011

Abstract Over the past decade, a large number of strategies and technologies have been developed to reduce heart failure progression. Among these, cardiac tissue engineering is one of the most promising. Aim of this study is to develop a 3D scaffold to treat cardiac failure. A new three-block copolymer, obtained from δ-valerolactone and polyoxyethylene, was synthesised under high vacuum without catalyst. Copolymer/gelatine blends were microfabricated to obtain a ECM-like geometry. Structures were studied under morphological, mechanical, degradation and biological aspects. To prevent left ventricular remodelling, constructs were biofunctionalises with molecularly imprinted nanoparticles towards the matrix metalloproteinase MMP-9. Results showed that materials are able to reproduce the ECM structure with high resolution, mechanical properties were in the order of MPa similar to those of the native myocardium and cell viability was verified. Nanoparticles showed the capability to rebind MMP-9 (specific rebinding 18.67) and to be permanently immobilised on the scaffold surface.

C. Cristallini (✉) · G. D. Guerra
Institute for Composite and Biomedical Materials, C.N.R., U.O.S. of Pisa, Largo Lucio Lazzarino, 56122 Pisa, Italy
e-mail: caterina.cristallini@diccism.unipi.it

M. Gagliardi · N. Barbani
Department of Chemical Engineering, Industrial Chemistry and Materials Science, University of Pisa, Largo Lucio Lazzarino, 56122 Pisa, Italy

D. Giannessi
Institute of Clinical Physiology, C.N.R., Via Giuseppe Moruzzi 1, 56124 Pisa, Italy

1 Introduction

One of the major causes of morbidity and mortality in the industrialized world is myocardial infarction. In the most severe cases the only possible treatments, such as mechanical support based on left ventricular assistance devices or cardiac transplantation, present important limitations. For this, there is an urgent interest in the identification of new strategies able to treat efficiently cardiac pathology. A promising method is myocardial tissue engineering where a scaffold can provide mechanical support to damaged tissues and mainly instructs stem cell, both seeded and in situ recruited, towards a correct morphogenesis of cardiac tissue [1]. A crucial problem in myocardial tissue engineering is that cells have to be inserted in tissue-engineered devices. Although cardiomyocytes are the principal component of the cardiac tissue, endothelial cells, fibroblasts, smooth muscle cells, neural cells, and leukocytes comprise about 70% of the total cell number in the working myocardium. A possible solution can be the use of stem cells or the insertion of cardiomyocytes [2]. The identification of a suitable cell source for tissue-engineered myocardial patches has been a severe challenge for many years. Indeed, allogenic cells are easy to obtain but could cause immune suppression; autologous cells do not show immunologic issues but are more difficult to obtain and expand in cell culture [3]. A great variety of polymeric materials, including synthetic or natural polymers and hybrid materials, has been explored [4]. The last class also comprised bioartificial materials, considered interesting because they can combine together the best properties of both components, mainly in terms of biocompatibility [5–7]. The basic concept is that, anticipating at molecular level the interaction between synthetic and natural components, it is possible to foresee a better integration with the natural tissue in

Published online: 06 December 2011

respect to an artificial material, as verified for a large range of polymeric systems able to mimic the extra-cellular matrix (ECM) of different tissues such as bone and myocardium [8, 9]. The optimal scaffold to engineer cardiac muscle tissue has not yet been found because of needs for satisfy the large repertory of requirements that a system, designed to substitute structure and function of cardiac ECM, must possess but recent papers conclude that research can lead to find it in a short time [4, 10, 11]. Basic scaffold requirements are biocompatibility, biodegradability, and mechanical properties with a great compliance toward the natural tissue. Moreover, porosity and micro architecture of the scaffold are additional aspects to stimulate cell migration, growth, and vascularisation as well as provide nutritional conditions for cells. One approach relies on attempts to mimic the micro architecture of tissues and the microenvironment around cells within the body [12–14]. The development of scaffolds with controlled architecture and specific surface topography, obtained through several techniques such as selective laser sintering [15, 16] and soft lithography [14], have been already described in literature. Recently the authors prepared and characterised three-dimensional microfabricated and bioartificial scaffolds through soft lithography able to mimic the cardiac ECM architecture [17].

Finally, an engineered construct has to be biomimetic, stimulating precise reactions at a molecular level to direct cell behaviour in terms of adhesion, differentiation, stem cell recruitment, thanks to the presence of specific biochemical and/or topological signalling at nano-scale level [18]. To mimic the native tissue structures nanotechnologies can be merged with biomaterials [19]. Our research group proposed for the first time molecular imprinting (MI) as a new nanotechnology for the preparation of advanced synthetic structures supporting cell adhesion and proliferation [20]. The MI technique allows obtaining synthetic polymers, named molecularly imprinted polymers (MIPs), capable to bind selectively a specific substance (template) [21–23]. The main applications of MIPs include analytical separation, artificial immuno-mimetic, antibody-mimetic systems, and biomimetic sensors; in recent years, our research aimed at developing novel applications of MIPs with regard to biomaterials and tissue engineering [24–26]. The use of MIPs in tissue engineering improves the scaffold performances adding complementary and selective sites towards specific peptide sequences present in the extra-cellular proteins. It can increase cell adhesion and growth, as well as stem cell recruitment.

Preliminary in vitro cell culture tests demonstrated the ability of functionalized materials with imprinted nanoparticles towards both fibronectin GRGDS and laminin YIGSR sequence to promote cell adhesion, proliferation, and differentiation [27, 28].

Poly(ester–ether–ester) tri-block copolymers have been proposed as bioresorbable materials since many years [29, 30]. Since the not-catalysed synthesis was developed in our laboratories [31–33], these copolymers were tested for cell adhesion and proliferation and cytotoxicity [34, 35], as well as for cytocompatibility and hemocompatibility [36, 37]. In vitro degradation of the copolymers, both in the presence and in the absence of cells, was also tested [38]. Results showed that degradation products did not alter endothelial metabolism [39] and modulated the endothelin release by human umbilical vein endothelial cells, with no significant alteration of the vasoconstrictor-vasodilator balance [40]. Recently, microspheres of poly(ester–ether–ester) and of polyurethanes containing poly(ester–ether–ester) chains were fabricated and tested as devices for the controlled release of Paclitaxel, an anti-mitotic drug [41]. Some authors studied a low molecular weight and temperature-sensitive hydrogel PVL–POE–PVL with vascular endothelial growth factor (VEGF) for the controlled local release of the cytokine [42].

The cardiac ECM plays a fundamental role in wound repair post-myocardial infarction and its degradation and remodelling is controlled by matrix metalloproteinase (MMPs) proteolytic system. Cardiac tissue repair following MI is a complex process involving three overlapping phases: inflammation process, granulation tissue formation and late remodelling that can ultimately lead to a progressive decline of heart contractile function. Specific spatial and temporal profiles of MMPs and their inhibitors (TIMPs) were described for each of these phases [43]. In particular, the MMP-9 is over-expressed and its active form increases mainly during the first and second phase in infarcted myocardium. Activation of MMP-9 can stimulate detrimental effects on the healing process while the TIMPs expression, participating in the maintenance of normal cardiac functional integrity, seems to be reduced following MI. Studies on animal models have demonstrated the efficacy of some pharmacological agents (such as ramapril, valsartan, propanolol) in modulating the MMPs/TIMPs balance [44]. However, the main challenge is to target a specific element among the broad spectrum of different enzymes belonging to the MMP family [43]. In this context, our idea was to evaluate the possibility of using the MI technology to obtain a potential therapeutic tool, innovative in respect to the existing chemical agents, able to recognize selectively a specific MMP at a particular time step.

With the aim of developing new biodegradable multifunctional scaffolds replicating cardiac ECM structure also reducing or preventing the left ventricle remodelling [45–48], we planned a framework consisting of different phases. At first, novel microfabricated systems, composed of synthetic or bioartificial materials, were prepared and characterised. This phase consists of three specific tasks:

(i) synthesis and characterisation of new biodegradable poly(ester–ether–ester) copolymers (PVL–POE–PVL) obtained by ring-opening mechanism in the complete absence of catalyst; (ii) processing of copolymer, also in combination with a biological component, in a ECM-like microstructure specifically designed for this purpose; (iii) physicochemical, mechanical, and biological characterisation of polymeric manufacts. Secondly, microfabricated systems were modified by adding molecularly imprinted nanoparticles (MIPs) able to recognize a specific metalloproteinase (MMP-9). This phase includes two principal tasks: (i) synthesis and characterisation of MIPs towards MMP-9; (ii) deposition of MIPs onto microfabricated structure surface.

2 Experimental

2.1 Materials

To obtain three-blocks copolymers, δ-valerolactone (VL, Aldrich), and poly(ethylene glycol) standards (Aldrich) with number-average molecular weight of 20,000 Da (PEG20k), and 35,000 Da (PEG35k) were used as reagents. Tin(II) 2-ethylhexanoate (Aldrich) was used as catalyst for preliminary syntheses. VL was purified to remove the inhibitor using a packed column containing the inhibitor remover (Aldrich), then dried in vacuum oven at low temperature and stored at −20°C. PEGs were dried under-vacuum to remove water content and stored in a desiccant container at room temperature. Tin(II) 2-ethylhexanoate was used without any further purification.

Gelatine A from porcine skin (GEL, Aldrich) was used as received to obtain bioartificial materials.

Poly(dimethylsiloxane) prepolymer (Sylgard 184 kit) was used to prepare the microfabricated mould.

For nanoparticle synthesis, methacrylic acid (MAA, Sigma Aldrich), poly(ethylene glycol) ethyl ether methacrylate ((PEG)EEMA, Sigma Aldrich, average molecular weight 246 Da) as monomers and thrimethylolpropane thrimethacrylate (TRIM, Sigma Aldrich) as cross-linker were used. Monomers were purified and stored with the same procedure used for VL while TRIM was used as received. Sodium metabisulfite (Aldrich, $Na_2S_2O_5$) and ammonium persulfate (Aldrich, $(NH_4)_2S_2O_8$) were dried and used as radical initiator of the reaction. Human MMP-9 (92 kDa, R&D Systems Inc.) metalloproteinase enzymes were used to obtain MIPs.

For MTT test (3-(4,5-dimethylthiazol-2-yl)-2,5-diphenyl tetrazolium bromide assay), Dulbecco's modified Eagle's medium (DMEM, Cambrex) containing 10% v/v fetal bovine serum (FBS, Cambrex), C2C12 line cells (European Collection of Cell Culture), and ELISA reader (BioRad mod.450) were used.

Dimethylsulfoxide (DMSO), chloroform (CHL), dichloromethane (DCM) methanol (MeOH), ethanol (EtOH), acetone (ACT), tetrahydrofuran (THF), isopropanol (ISP), acetonitrile (ACN), hydrochloric acid (HCl) all purchased from Carlo Erba Reagenti and with HPLC purity degree, and bidistilled water (Direct-Q UV system, Millipore) were used as solvents. A phosphate buffered saline (PBS, Sigma) solution with pH 7.4 was used as reaction medium to prepare nanoparticles and for degradation tests.

2.2 Synthesis of three-block copolymers

Preliminarily, a series of three-blocks copolymer syntheses were performed by varying the PEG molecular weight and the VL/PEG percentage weight ratio (90/10, 85/15, 80/20) to obtain tunable systems in terms of degradation and mechanical properties. Syntheses were carried out both in the presence and in the complete absence of catalyst.

Ring-opening polymerisations in the presence of the catalyst (0.11% w/w) were performed under dry N_2 atmosphere at 100°C for 24 h. Reaction products were purified by repeated precipitation into bidistilled water from DMSO solution, filtered and dried under-vacuum to completely remove residual water. Syntheses in the presence of catalyst were carried out mainly for a rapid and efficient preliminary evaluation of the newly-synthesised materials, then polymerisations were performed using a special reaction apparatus specifically designed for the synthesis of this kind of copolymers, following a procedure already optimized in the past by researchers of our group for analogues copolymers [31–33].

Polymerizations were carried out in glass tubular reactors directly connected to a vacuum line. The line is provided of a turbo-molecular pump (Oerlikon Leybold Vacuum) able to reach pressures up to 10^{-9} mmHg. The measured volume of VL was dispensed into a glass tube containing the pre-weighed amount of PEG, the reaction mixture was connected to the vacuum line for 24 h and maintained at maximum vacuum (about 10^{-4} mmHg). The tube was sealed off using a Swagelok® valve and placed in oven at 100°C. After 1 week, the reactor was opened and the mixture dissolved in CHL. Products were quantitatively recovered by precipitation in excess of MeOH, washed several times with aqueous MeOH and dried in vacuum at 37°C. Under-vacuum syntheses were carried out three times for each material in order to evaluate the repeatability of the preparation. Preliminary Fourier-transform infrared (FT-IR) and differential scanning calorimetry (DSC) analyses were performed onto obtained products showing no differences in the results.

2.3 Preparation of cardiac ECM-like microfabricated polymeric systems

In this work, a rectangular cell configuration mimicking cardiac ECM for fabrication of scaffolds was used (Fig. 1). The design of the geometry, already described in detail in a previous article [17], was obtained directly from optical microscope images of transversal and longitudinal sections of porcine cardiac tissue. Specimens of the tissue, both decellularized and not, were embedded in paraffin and sectioned by rotary microtome for staining. From tissue cross sections, micrometric parameters were obtained (cardiomyocyte dimensions and thickness of connective tissue surrounding bundles of muscle fibres). On the basis of this evaluation, the micro-pattern model, well fitting the cardiac ECM geometry and simple to be transferred to microfabrication techniques, is characterised by rectangular cavities (500 μm × 100 μm), able to hypothetically locate 2–3 cardiomyocytes. The meshed structure also presents thick lines of 30 and 70 μm corresponding to different contents of connective tissue components (mainly collagen I).

The 2D CAD model of the geometry was obtained using SolidWorks (Dassault Systèmes, SolidWorks Corp.). Master geometry was obtained through the soft lithography technique, reproducing the single-cell geometry to generate a micro-patterned scaffold with 5 cm × 2.5 cm in dimension, suitable for a wide range of characterisations (i.e., bioreactor). A poly(dimethylsiloxane) mould was produced, following the standard procedure indicated for the Sylgard kit. Mould was detached from the master and used as substrate for the deposition of the polymeric solution.

Different polymeric solutions composed of copolymer or bioartificial blends were prepared. Microfabricated systems of pure PVL–POE–PVL, were obtained pouring 1 ± 0.2 ml of polymeric solution in CHL (15% w/v) using a micropipette. Solutions were spread onto the mould and the excess of solution was removed to obtain thin and porous structures by casting of the solvent in a vented oven at controlled temperature (40°C for 2 h). The complete removal of the organic solvent was verified by FT-IR analysis.

Microfabricated bioartificial systems were obtained by phase inversion for controlled casting from a ternary solvent blend composed of a solution of PVL–POE–PVL in DCM (20% w/v), ACT and a solution of GEL in water (10% w/v). The percentage volumetric composition of the solvent mixture was 52/42/6, respectively. The bioartificial blend PVL–POE–PVL/GEL (90/10 w/w) was homogeneously distributed over the PDMS mould and casted at 35°C in vented oven. Microfabricated materials obtained were gently detached at the end of the casting procedure.

2.4 Characterisation of microfabricated systems

2.4.1 Morphological and physicochemical analyses

Morphological analysis was carried out onto samples coated with 24 k gold in a vacuum chamber through scanning electron microscope (SEM) using a JEOL T-300 instrument.

Differential scanning calorimetry was carried out in dry state in triplicate with a DSC7 apparatus (Perkin Elmer). Samples (5 ÷ 9 mg) were sealed in aluminium pans and analysed in the temperature range from −30 to 150°C under N_2 flux (temperature ramp 10°C/min). PVL–POE–PVL, PEG35k standard, homopolymer PVL, a mechanical blend PVL/PEG in the form of thin films obtained by casting were analysed.

Gel permeation chromatography (GPC) was performed to evaluate macromolecular compositions and molecular weights of the products using a Perkin Elmer series 200 apparatus equipped by refractive index and UV detector ($\lambda = 245$ nm), a ResiPore column (300 × 7.5 mm, particle size 3 μm) with THF as mobile phase (flow 1 ml/min). Samples were dissolved in CHL (0.2% w/v) and measurements were acquired on the basis of a calibration curve obtained from polystyrene standards dissolved in CHL and the TurboSec software (PerkinElmer).

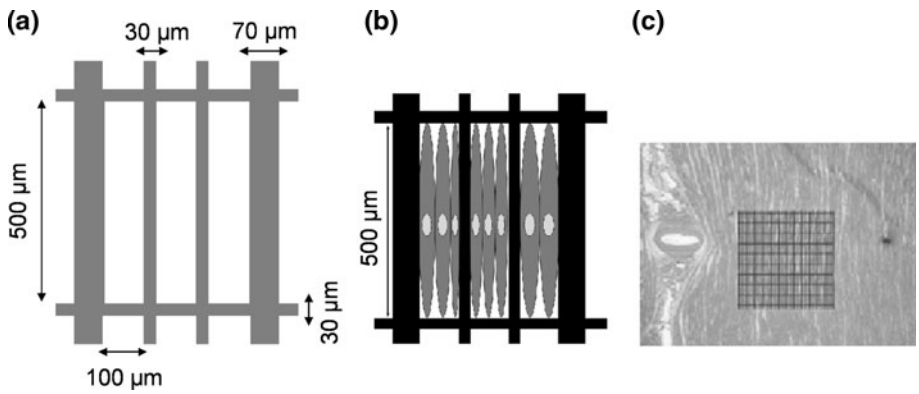

Fig. 1 Design of the ECM-like structure of the microfabricated polymeric systems: **a** simplified geometric scheme of a single-cell of the structure with dimensions; **b** hypothetical cardiomyocytes arrangement within cells; **c** superposition of the designed ECM-like structure on the native cardiac tissue

Total reflection FT-IR spectra were obtained through Spectrum One FT-IR Spectrometer (Perkin Elmer). Samples of copolymers obtained both in the presence and in absence of catalyst and samples of corresponding homopolymers were analysed to verify the presence of characteristic peaks of the components.

2.4.2 Mechanical characterisation

Mechanical properties were evaluated by DMA 8000 (Perkin Elmer). A set of mechanical analyses (tensile, strain scan and multi-frequency tests) was carried out to evaluate elastic modulus and complex dynamic modulus in strain and in multi-frequency scans. Quasi-static tensile tests were performed with 0.01 s^{-1} strain rate; strain scan tests were performed applying a stepped strain (from 0.01% to 30%) in 0.01 s per step; multi-frequency tests were performed on pre-deformed samples (5% in respect to the starting length) by applying a cyclic strain (10% referred to the pre-strain) at three different frequencies (1, 2, 3 Hz). Tests were carried out in triplicate.

2.4.3 Degradation tests

Degradation tests were carried out in triplicate by immersing in PBS microfabricated specimens of pure copolymers and bioartificial materials. Samples were maintained at 37°C under gentle mechanical stirring. After 6, 12, 30, 40, 50 days samples were removed from the solution, rinsed with distilled water, dried, and weighed. The extent of degradation was calculated according to Eq. 1

$$w_L = \frac{w_0 - w(t)}{w_0} \cdot 100 \quad (1)$$

where w_L is residual weight percentage, w_0 is the starting dried weight and $w(t)$ is the dried weight of the sample after degradation.

2.4.4 Sterilization and cytotoxicity tests

Sterilization tests were performed onto three samples for each typology of microfabricated systems to evaluate the stability of materials after sterilization procedure. Squared samples (1 cm × 1 cm) were immersed in the sterilization medium (70% EtOH aqueous solution) for 30 min by changing the medium after 15 min. Then, samples were dried and placed under UV light for 15 min on each sample side to complete the sterilization procedure. Finally, samples were weighed to evaluate the loss in weight following sterilization.

Preliminary cell viability tests were performed by means of MTT assay on microfabricated samples obtained by pure copolymers and bioartificial systems. Samples (1 cm × 1 cm) were sterilised as described. Microfabricated systems were placed in 24-well plates and seeded with a C2C12 cell suspension (cell density 10^5 cells/ml) in DMEM containing FBS. Cells were also cultured directly on the wells as control. Cell culture was carried out in a humidified atmosphere containing 5% CO_2 at 37°C for 72 h. After 24 and 72 h of incubation, cell viability was measured by MTT assay as follows. After each time, MTT (1 mg/ml in PBS) was added to the medium in volumetric ratio 1:10 and samples were further incubated for 4 h at 37°C. The medium was removed and purple formazan crystals were solubilized with 200 ml of acidic ISP (0.04 M HCl in ISP) at room temperature. Optical density (OD) at a $\lambda = 570$ nm was determined using an ELISA reader. In order to carry out a statistical analysis (ANOVA), seven tests were performed onto bioartificial blends in form of membrane and microfabricated structure.

2.5 Synthesis of imprinted nanoparticles towards MMP-9 (MMP-9/MIPs)

Molecularly imprinted nanoparticles able to recognize MMP-9 were synthesised using precipitation polymerisation method. The synthesis was performed by radical polymerisation of MAA and (PEG)EEMA in the presence of TRIM. Human MMP-9 (total), also known as gelatinase B and secreted as a 92 kDa zymogen, was also added in the reaction feed.

The template molecule (MMP-9) (40 ng) was suspended in PBS solution by adding 1 ml into the vial and mix gently. MAA and (PEG)EEMA (percentage molar ratio MAA/(PEG)EEMA 75/25), TRIM (20% mol/mol in respect to the total amount of monomers) were inserted in reaction tube and mixed at 37°C. Thereafter, the MMP-9 solution was added into tube reactor containing reagents, operating under dry N_2 flux and maintaining reaction mass at 37°C. When the solution became clear, 0.05 M of $Na_2S_2O_5$ and $(NH_4)_2S_2O_8$ already dissolved in PBS (1 ml) at 37°C were added to the solution under agitation. Tube reactor was sealed off and the polymerisation was carried out for 3 h ensuring a light constant stirring at 37°C. The solid product obtained in form of nanoparticles was separated by the PBS solution by ultracentrifugation (Mikro 200 Hettich Zentrifugen) with 14,000 rpm for 15 min. Then, nanoparticles were washed by bidistilled water for three times and dried in vented oven at 37°C. The template enzyme was removed by several washing in PBS solution; at each extraction cycle nanoparticles suspension was ultracentrifuged and supernatant withdrawn and collect to successive HPLC analysis in order to determine amount of MMP-9 extracted. Not-imprinted nanoparticles (CPs) were

prepared as control in the absence of MMP-9 and treated in the same way.

2.6 Characterisation methods of MMP-9/MIPs

2.6.1 Recognition experiments

To evaluate the binding capacity of MMP-9 imprinted nanoparticles (MMP-9/MIPs), 30 mg of MIPs or CPs were placed in eppendorf and incubated in 1 ml of rebinding solution (10 ng of MMP-9 in 1 ml of PBS) under gentle agitation at 25°C for 2 h. MIPs and CPs suspensions were ultracentrifuged and supernatant withdrawn from each eppendorf was analysed by HPLC to evaluate the residual amount of MMP-9 in both cases. To determine MMP-9 amount both in extraction and rebinding solutions, a C18-Synergy Hydro-RP (250 × 3 mm, 4 μm, Phenomenex) column was used, ACN/water (80/20 v/v) as mobile phase (flow rate 0.8 ml/min), UV detector was set at 280 nm and injections were performed autosampling 10 μl of different solutions.

A series of parameters were calculated as indicated in following equations:

$$\text{MMP-9retained} = \frac{\text{ng MMP-9final}}{\text{ng MMP-9initial}} \times 100 \quad (2)$$

$$\text{MMP-9extracted} = \frac{\text{ng MMP-9extracted}}{\text{ng MMP-9retained}} \quad (3)$$

$$\text{Rebinding capacity} = \frac{\text{MMP}-9\text{bound by MIP} - \text{MMp-9bound by CP}}{\text{Nanograms of MMP-9retained}} \times 100 \quad (4)$$

$$\text{Specific rebinding} = \frac{\text{ng MMP-9bounnd by MIP} - \text{MMp-9bound by CP}}{\text{Grams of polymer}} \quad (5)$$

Recognition tests were performed onto three series of nanoparticles obtained in three different syntheses. For each product, tests were performed in triplicate and then results following reported are mean values of nine different tests. However, no relevant differences were detected between products obtained in different syntheses.

2.6.2 Zymography analysis

To evaluate the activity of MMP-9 after rebinding tests, the zymography assay of rebinding solutions after contact with MIPs and CPs was performed. MMP activity in different enzyme solutions was analysed using gelatin zymography, performed by standard procedures using a sodium dodecylsulfate/polyacrylamide gel electrophoresis matrix containing gelatin (1 mg/ml). The activity of the bands was quantified by densitometry (ImageQuant, Molecular Dynamics). The zymograms were analysed for a lytic band corresponding to standards for the proenzyme (92 kDa) form of MMP-9. The values obtained for MMP activity for each sample were normalized for their protein concentration using HPLC assay. Tests were performed in triplicate. Once normalized, results of MMP-9 activity in solutions in contact with MIPs and CPs were compared.

2.7 Biofunctionalisation of MMP-9/MIPs on microfabricated systems

MMP-9/MIPs spray deposition onto microfabricated systems was optimized to avoid any alteration of the polymeric structure. Particles were grinded, dispersed in EtOH aqueous solution (70% v/v) and sonicated with a Ultrasonic 06 apparatus (Falc) for 30 min, then were mechanical stirred and nebulisated on both sides of the microfabricated system. Finally, systems were exsiccated at 25°C.

After the nanoparticle deposition, the MIPs-modified microfabricated biodegradable systems were subjected to stability tests in order to verify the MIPs adhesion. Samples were immersed in PBS solution and maintained under stirring for 3 days, then dried and analysed by SEM.

3 Results and discussion

3.1 Synthesis of three-blocks copolymers and characterisations

Six different copolymers, obtained by varying the length of the PEG chain and the weight ratio between components, were obtained in the presence of catalyst. At first, processability was verified. Copolymers with VL/PEG ratios 80/20 and 90/10 showed that it was not possible to obtain consistent and reproducible products. For this reason, these compositions were not considered for further tests. On the contrary, copolymers with composition 85/15 obtained with both PEGs were well processed into thin films and preliminarily characterised. On the basis of this aspect, the synthesis in absence of catalyst was carried out only for copolymers with composition 85/15.

In Table 1 results of tensile tests and in vitro degradation analysis onto copolymers PVL–POE–PVL 85/15, obtained using both PEG20k and PEG35sk, are reported. Elastic modulus of materials containing PEG35k were smaller than those obtained with materials containing PEG20k, resulting more similar to mechanical values reported in literature for myocardial native tissue [13]. In addition, stability in PBS of copolymers with PEG35k was

Table 1 Elastic modulus evaluated through tensile tests for copolymers with VL/PEG percentage ratio 85/15 obtained both with catalysed and not-catalysed synthesis

Copolymer	Catalyst	Elastic modulus (MPa)	w_L (Eq. 1)
PVL–POE–PVL 85/15 (PEG20k)	Yes	65.8 ± 1.2	20.5 ± 1.1
	No	52.4 ± 2.5	24.1 ± 1.2
PVL–POE–PVL 85/15 (PEG35k)	Yes	9.1 ± 0.3	8.1 ± 0.6
	No	9.0 ± 0.1	8.2 ± 0.8

significantly higher than those containing PEG20k, independently by the presence of the catalyst in the reaction feed. For this reason, further characterisations were carried out only onto copolymers containing PEG35k (copolymer obtained in the presence of the catalyst was considered only as reference system).

Fourier-transform infrared spectra of the copolymer showed the presence of the typical bands of PVL and PEG homopolymers (stretching of C=O at 1,723 cm^{-1} and stretching mode of C–O at 1,165 cm^{-1} typical of PVL; stretching of C–O–C at 1,065 cm^{-1} typical of PEG), confirming for each of them their ester-ether structure (Fig. 2a). DSC thermograms for copolymers, homopolymers (PVL and PEG35k) and a mechanical blend (85/15 w/w) are reported in Fig. 2b. In the trace of the mechanical blend, the presence of two distinct peaks at the same temperatures was observed, corresponding to melting of pure homopolymers. On the contrary, for copolymers only one melting event was registered, indicating that the copolymerisation occurred. A decrease in the melting temperature for copolymers in respect of homopolymers was observed, in agreement with results obtained for similar block copolymers as reported in literature [31–33]. Considering the melting enthalpy, a reduction of the values was observed for copolymers (96 and 102 J/g for catalysed and not-catalysed respectively versus 150 J/g for PVL and 280 J/g for PEG35k). This result could be explained with the hypothesis that the segment that crystallises first (PVL) has a tendency to freeze the whole structure, thus imposing either imperfect crystallization or smaller crystallites onto the POE segment. Tests were performed in dry state but a more exhaustive characterisation in wet conditions maybe necessary, as suggested in the work of Zeugolis and Raghunath [49].

Gel permeation chromatography analysis showed that the weight average molecular weight of the copolymer obtained both in catalysed and in uncatalysed reaction was similar (1.45×10^5 and 1.42×10^5 Da, respectively). In addition, the macromolecular composition was evaluated (VL/PEG35k weight ratios were found to be 76/24 and 75/25, respectively). This result allows evaluating the VL conversion at the end of the reaction (89.4 and 88.2%, respectively), confirming that the under-vacuum reaction scheme designed ad hoc showed a great efficiency.

Considering that the physicochemical behaviour of copolymers obtained through both reaction schemes did not show substantial differences, bioartificial materials were prepared using the copolymer obtained in the absence of catalyst. It ensures a greater biocompatibility of the final product, considering that traces of toxic catalyst could persist also after a deep purification.

DMA tests allowed evaluating mechanical properties of the materials. Elastic modulus obtained in tensile tests were already reported in Table 1 and discussed. Results of dynamic tests are summarised in Fig. 3. In multi-frequency tests (Fig. 3a), E' did not show significant differences by varying the frequency, both for synthetic and bioartificial samples. Results of E'' are not reported, however, values were found to be very low in respect of E', indicating a predominant elastic behaviour. Storage modulus resulted in the order of MPa for copolymer samples, with values

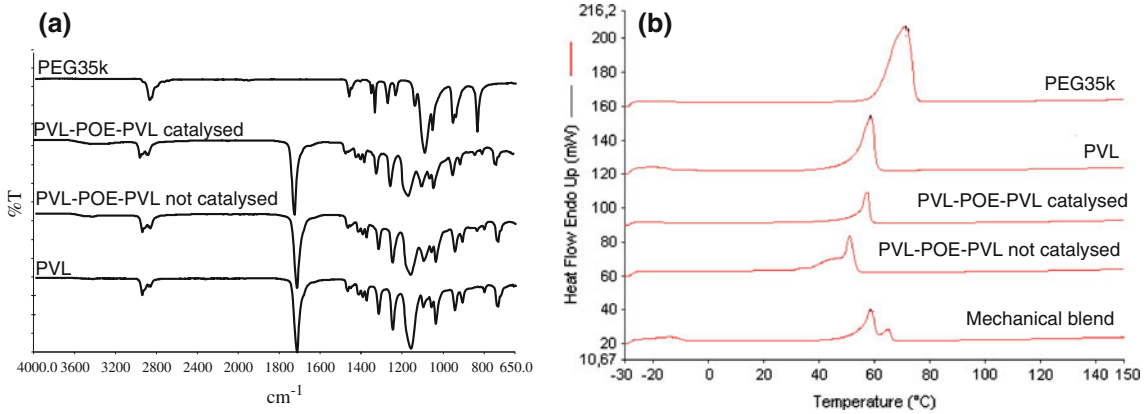

Fig. 2 Physicochemical characterisation: **a** FT-IR spectra of copolymers 85/15 obtained with and without catalyst compared with spectra of homopolymers and **b** DSC second scan thermograms, obtained in dry conditions, of copolymers 85/15 compared with thermograms of homopolymers and mechanical blend (85/15 weight composition), scan rate 10°C/min

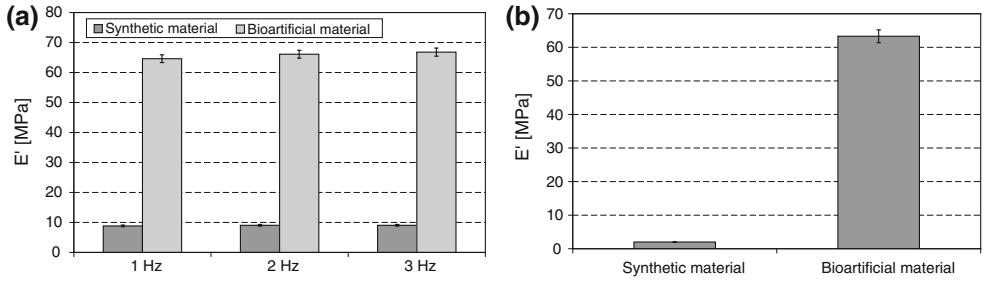

Fig. 3 Results of mechanical analysis onto copolymer 85/15 obtained through under-vacuum synthesis and the respective bioartificial blend: storage modulus (E') **a** obtained in multi-frequency tests (pre-strain 5% and cyclic strain 10% on the pre-strain value) and **b** in strain scan tests (stepped strain from 0.01 to 30% in 0.01 s per step); values represent the mean ($n = 3$) ± STD

similar to the native cardiac tissue [46]. For bioartificial specimens higher values were registered (68.4 ± 1.0 MPa). Strain scan analysis (Fig. 3b) confirmed the previous results. In both tests, the bioartificial system showed higher values of E' than the pure copolymer. However, results are compatible with specific application considering that measurements were performed in the dried state rather than in aqueous conditions.

Differential scanning calorimetry analysis was carried out onto the bioartificial system containing GEL (10% w/w in respect to the synthetic polymer content). Thermograms of the pure copolymer and of the bioartificial system did not show significant differences (melting enthalpies were 102 and 99 J/g, respectively, melting temperatures were 51 and 57°C).

Another important aspect of this work was the design and fabrication of scaffolds with rectangular-meshed configuration approximating cardiac ECM geometry. In Fig. 4 the microstructure obtained by soft lithography for the scaffold based on PVL–POE–PVL copolymer shows a high correspondence with the predefined geometry. The accuracy of replication is confirmed by the measured values of the cell profiles (490 ± 5, 99 ± 3, 71 ± 2, and 35 ± 2 μm) that are very similar to the geometry of the model used (500, 100, 70, and 30 μm).

To evaluate the kinetics of in vitro degradation between microfabricated systems based on pure copolymer and those based on PVL–POE–PVL/GEL blend, mass loss of both materials after incubation in PBS solution was evaluated up to 40 days. For both systems, a constant and gradual weight reduction was observed although bioartificial systems showed a faster degradation rate as compared to pure copolymer systems (Fig. 5a). After 40 days, microfabricated samples of pure copolymer showed 10% mass loss while a value of mass loss of 37% was registered for bioartificial structure. The higher degradation rate for bioartificial materials have to be rationally ascribed to a release, even is gradual, of GEL component during degradation time.

The evaluation of the mass loss after sterilization was carried out and not significant decrease in the sample weights were detected, for both synthetic and bioartificial materials, resulting smaller than 2%.

Preliminary studies of cytocompatibility on materials obtained were performed. As the most significant example of in vitro cell culture results, absorbance values measured by MTT tests (Fig. 5b) for a microfabricated bioartificial system were compared with those obtained with a material having the same chemical composition (PVL–POE–PVL/GEL 90/10 w/w) but not microfabricated. Both systems did

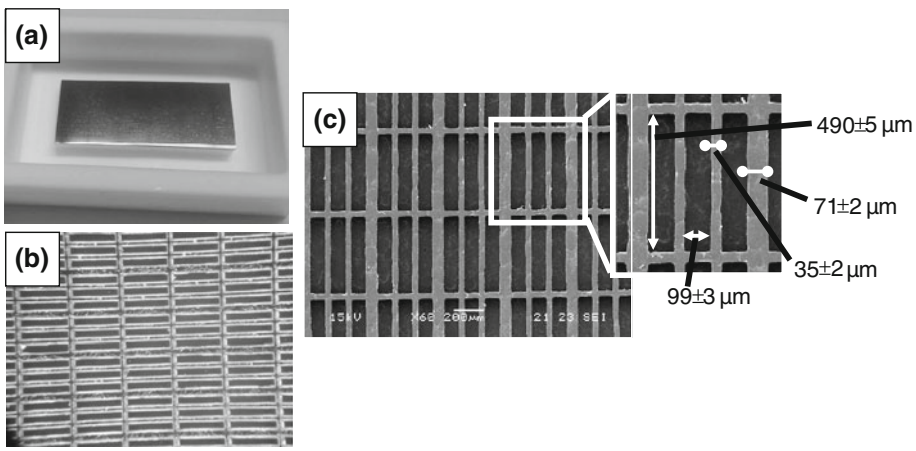

Fig. 4 Microfabrication: **a** the Teflon container where the silica master (5 cm × 2 cm) used to prepare silicon moulds was stuck; **b** SEM image of the PDMS mould used to prepare samples; and **c** SEM image of the microfabricated system surface for PVL–POE–PVL 85/15, obtained through under-vacuum synthesis and particular of a single-cell of the structure with line dimensions

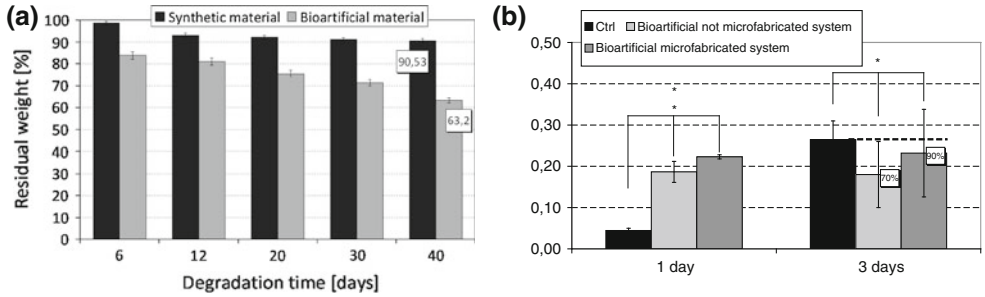

Fig. 5 **a** In vitro degradation test onto the pure copolymer with composition 85/15 obtained through under-vacuum synthesis and the respective bioartificial blend (90/10), residual weight of samples after degradation in PBS solution; **b** In vitro cell viability using C2C12 cells by MTT assay, comparison between values of absorbance for PVL–POE–PVL/gelatin (90/10) membranes having micro patterned surface and not with respect to the tissue culture plate as negative control (nCtrl), values represent the mean ($n = 7$) ± SD; ANOVA test, significance level referred to nCtrl: * $P < 0.05$; ** $P < 0.01$

not show significant effects on the cytotoxicity ($P < 0.05$). However, cell viability measured after 72 h respect to negative control was 70% ($P < 0.05$) for not microfabricated materials and 90% ($P < 0.05$) for the microfabricated system. Such important result seems to suggest a positive effect of anisotropic structure of the polymeric material on cell viability.

3.2 Synthesis and characterisation of MIPs

A crucial objective of this work was to develop a scaffold addressing an important strategy of therapies in human cardiology to restore the correct equilibrium MMPs/TIMPs. Towards this goal, we thought to apply MI technology for the production of nanoparticles able to remove, in a controlled extent, MMP-9 involved in the early adverse phases of cardiac repair. The presence of complementary nanosites on the particle structure should ensure a high-selective removal, not involving other molecules or enzymes present in the cardiac microenvironment. The synthesis of nanoparticles was carried out selecting two monomers, MAA and (PEG)EEMA, the first because is well known efficient monomer in MI [50], the second because contains a short chain of PEG exposed able to prevent inflammatory reactions and removal by RES. In addition, synthesis was performed using two catalysts that permit to carry out the reaction at 37°C and for 3 h, with the benefit of preserving as much as possible the bioactivity of the enzyme.

Concerning the characterisation of MIPs imprinted with MMP-9, carried out by HPLC, the amount of the MMP-9 contained in the final product, calculated as the difference between the amounts contained initially and the content found in reaction mixture, is reported in Table 2 as percentage of entrapped enzyme according to the equations indicated in experimental section. MMP-9/MIPs exhibited a good capability of entrapping the template molecule, resulting in 56.95% encapsulation efficiency. Since high cost and low availability of these enzymes, this result underlines the effectiveness of the followed experimental strategy. In the same table, the quantitative extraction of enzyme by repetitive PBS washing is reported as extracted fraction and the resulting value was 1.15%. As expected for MI of proteins [51], a permanent entrapment of the template in the polymer matrix, due to physical/chemical immobilization, occurred. A limited removal of biomacromolecule template was found but, for this specific application, this value can be considered acceptable. In fact, basing on the results reported in literature, a template removal from 50 up to 95% can be achieved for some proteins, but these efficiency levels are crucial mainly for conventional applications of MI such as analytical separations, enzyme-like catalysis or chemical sensors [21–23, 50].

Rebinding test was performed using an enzymatic solution with concentration 10 ng/ml (3.3×10^{-4} mg/g nanoparticles), both MIPs and CPs absorb quantitatively MMP-9, however a significant difference in rebinding behaviour was observed between, them showing a recognition factor of 1.34. This result confirms the effectiveness of MI technique to obtain specific binding sites on nanoparticles. Additionally, a particularly interesting result originates by the observation

Table 2 Characterisation of MIPs and CPs nanoparticles

Polymeric nanoparticles	% MMP-9 bound/MMP-9 rebinding solution	% MMP-9 retained (Eq. 2)	% MMP-9 extracted (Eq. 3)	Rebinding capacity (Eq. 4)	Specific rebinding (Eq. 5)
MIPs	10.40	56.95	1.15	1.15	18.67
CPs	7.80	–	–	–	–

that the percentage of enzyme extracted corresponds exactly to the percentage of enzyme rebound (1.15 is the value registered for both parameters) as indicated in Table 2. This means that the enzyme was able to occupy all the complementary specific sites on the MIPs.

Considering that mean values of MMP-9 concentration measured in rebinding solutions resulted in around 10 ng/ml, data obtained referred to rebinding capacity would be in agreement with those reported in literature for plasma MMP-9 following infarct myocardial (10–50 ng/ml) [52].

In addition, the possibility of using MIPs nanoparticles to attempt to remove specifically the enzyme correcting the in vivo MMP/TIMPS balance seem to be confirmed by these first experimental data. In particular, low percentage of enzyme rebinding represents a desirable result since the removal of high amount of enzyme in the microenvironment could actually be deleterious causing excessive depletion of enzymes responsible for the ECM cardiac regulation.

The activity of MMP-9 in different aqueous solutions was determined by zymography analysis. Washing solutions after polymerisation, extraction solutions and rebinding solutions both for MIPs and CPs were analysed and corresponding results were reported in Fig. 6. No evidence of activity was detected for the enzyme present in washing and extraction solutions (test tube indicated with 1, 2, 3, 4, in Fig. 6), reasonably due to drastic treatments that were carried out on nanoparticles imprinted with MMP-9. But a significant result was obtained comparing the evaluated OD of rebinding solutions after incubation with MIPs and CPs (test tube indicated with 5 and 6 in Fig. 6). MMP-9 activity normalized by enzyme content in rebinding solution was 4.20 for CPs and 14.83 for MIPs. These values were quantified using two independent assays, determining OD by zymography assay and enzyme concentration by HPLC. In most papers, enzyme concentration is quantified by direct ELISA measurements using standards curve, however the use of distinct methods is preferable and strengthens validity and accuracy of results obtained. The activity of MMP-9 measured in the solution after contact with imprinted nanoparticles was approximately 3.5 times higher than with not-imprinted particles. It could be explained with the previous contact of enzyme with MIPs structure that affected not only the amount of enzyme rebound but also its conformational state that determines its biological activity.

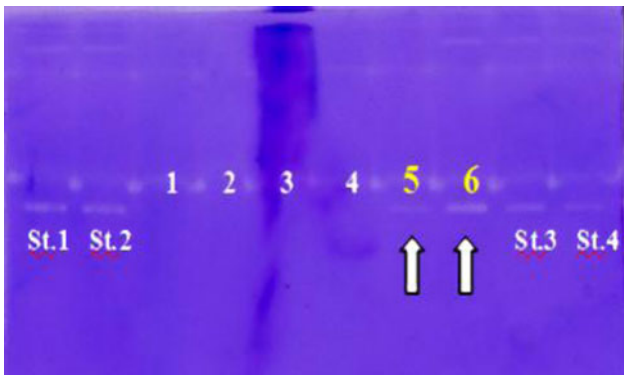

Fig. 6 Results of zymography analysis, evaluation of the OD for tested samples; standards are indicated as *St.x*, samples indicated with *5* and *6* are solutions withdrawn after rebinding tests for CP and MMP-9/MIP, respectively; no protease activity was visualised for CP (as control) and MIP polymerisation (*lanes 1* and *2*) and extraction solutions (*lanes 3* and *4*)

3.3 Biofunctionalisation of MMP-9 imprinted nanoparticles on microfabricated systems

Finally, in order to functionalize the microfabricated system by combination with MMP-9/MIPs, a procedure of deposition of nanoparticles onto the matrix was followed, as described in the experimental part. The choice of the solvent used to spread MIPs on the microfabricated system is critical to achieve a permanent physical immobilization until this will not degrade and nanoparticles will be cleared by physiological fluids. EtOH proved to be the most appropriate, as confirmed by SEM analysis and stability test. SEM image of scaffold after modification shows no alteration of the structure, in particular the rectangular-patterned surface is maintained (Fig. 7a). In addition, SEM analysis of microfabricated scaffold after stability test in aqueous environment allows ascertaining the efficacy of deposition procedure optimized (Fig. 7b). In particular, the solvent used allows a stable linking between nanoparticles and

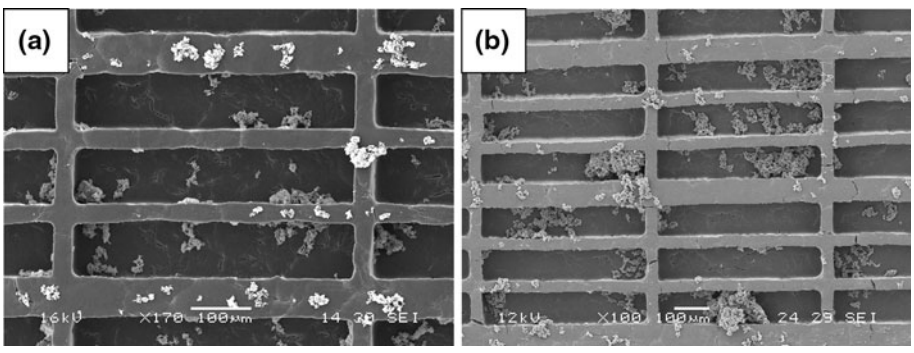

Fig. 7 Morphological analysis of the particle-loaded system obtained through SEM: surface of the system **a** after the MMP-9/MIP deposition and **b** after stability tests in PBS solution for 3 days

scaffold. It is important to underline that the effect of MMP-9 occurs mainly in the early remodelling phase (7–21 days) following infarction, while its role decreases in long term where MMP-9 returns to basal levels. Consequently, a loss of MMP-9/TIMP control, triggered by MIPs and due to degradation of scaffold supporting MIPs in a later stage, can be considered a desirable result for this specific application. In addition, morphological analysis of the multi-functional system showed the presence and distribution of nanoparticles both on the lines and on rectangular cavities. Different levels of particle aggregation were also found even if the nanosphere morphology is evident resulting in an approximately average diameter of 30 ± 10 nm.

On the basis of the results obtained by rebinding test previously discussed, the amount of MMP-9 rebound was 4.4×10^{-3} ng/cm^2 of scaffold surface. Although further study will be necessary to examine the entity MMP-9 inhibition in quantitative terms, values obtained by rebinding results seem to be compatible with low levels of these enzymes in a tissue.

These first results encourage us to continue in the direction of optimizing the production and characterisation of MIPs/scaffold systems in view of a future clinical utility in preventing dysfunction after myocardial infarction. However, a more extensive study of both the biological mechanisms involved in the activity of MMP/TIMP and therapeutic doses/activity are needed to make imprinting methodology from a simple proof of concept to a concrete therapeutic tool.

4 Conclusion and future developments

In this work it has been demonstrated the feasibility of manufacturing new multi-functional systems with a specific function at meso-, micro- and nano-scale level for cardiac tissue engineering.

However, for each level, further studies will be necessary to evaluate the efficacy of multi-functional systems obtained. Currently, the study of effects of only morphology functionalisation of the microstructures on the ability of stem cell differentiation in cardiac sense is underway, using in vitro cell cultures.

Moreover, recognition experiments on nanoparticles imprinted with MMP-9 demonstrated the specificity of these nanostructures towards the enzyme but a further aspect that is the evaluation of selectivity of imprinted nanoparticles toward TIMPs and other MMPs has to be performed yet.

Afterwards, 3D multi-layer scaffolds will be prepared by assembling of two or more microfabricated systems to achieve the requirements, also in terms of thickness, of an in vitro engineered myocardial tissue. Dynamic cell culture tests using a suitable bioreactor will be carried out to evaluate the effect of mechanical and electrical stimuli on the formation of construct.

In addition, the possibility to use the 3D multi-layer scaffolds for in vivo engineered myocardial tissue will be also evaluated after performing their biofunctionalisation with specific recruitment factors (e.g., SDF-1α).

Finally, in vivo experiments will allow evaluating the efficacy of multi-functional systems with synergic effect in both preventing left ventricular dysfunction and stimulate new cardiac tissue formation.

Acknowledgments Authors would acknowledge Dr. F. Boccafoschi (University of Eastern Piedmont "Amedeo Avogadro", Novara, Italy) for cytotoxicity tests and Dr. T. Prescimone (Institute of Clinical Physiology, National Research Council, Pisa, Italy) for zymography analysis. This work was financially supported by Italian Ministry of University and Research PRIN-2008 grant (Bioartificial stem cell niches for cardiac tissue engineering, 2010–2012).

References

1. Jawad H, Lyon AR, Harding SE, Ali NN, Boccaccini AR. Myocardial tissue engineering. Br Med Bull. 2008;87:31–47.
2. Zimmermann WH, Eschenhagen T. Cardiac tissue engineering for replacement therapy. Heart Fail Rev. 2003;8:259–69.
3. Leor J, Amsalem Y, Cohen S. Cells, scaffold, and molecules for myocardial tissue engineering. Pharmacol Ther. 2005;105:151–63.
4. Prabhakaran MP, Venugopal J, Kai D, Ramakrishna S. Biomimetic material strategies for cardiac tissue engineering. Mater Sci Eng C. 2011;31:503–13.
5. Giusti P, Lazzeri L, Lelli L. Bioartificial polymeric materials: a new method to design biomaterials by using both biological and synthetic polymers. Trends Polym Sci. 1993;1:261–7.
6. Cristallini C, Lazzeri L, Cascone MG, Polacco G, Lupinacci D, Barbani N. Enzyme-based bioartificial polymeric materials. The system a-amylase-poly(vinyl alcohol). Polym Int. 1997;44:510–6.
7. Cristallini C, Barbani N, Giusti P, Lazzeri L, Cascone MG, Ciardelli G. Polymerization onto biological templates, a new way to obtain bioartificial polymeric materials. Macromol Chem Phys. 2001;202:2104–13.
8. Guerra GD, Cristallini C, Rosellini E, Barbani N. A hydroxyapatite-collagen composite useful to make bioresorbable scaffolds for bone reconstruction. Adv Sci Technol. 2010;76:133–8.
9. Rosellini E, Cristallini C, Barbani N, Vozzi G, D'Acunto M, Ciardelli G, Giusti P. New bioartificial systems and biodegradable synthetic polymers for cardiac tissue engineering: a preliminary screening. Biomed Eng Appl Basis Commun. 2010;22:497–507.
10. Mukherjee S, Gualandi C, Focarete ML, Ravichandran R, Venugopal JR, Raghunath M, Ramakrishna S. Elastomeric electrospun scaffolds of poly(l-lactide-*co*-trimethylene carbonate) for myocardial tissue engineering. J Mater Sci Mater Med. 2011;22:1689–99.
11. Kai D, Prabhakaran MP, Jin G, Ramakrishna S. Guided orientation of cardiomyocytes on electrospun aligned nanofibers for cardiac tissue engineering. J Biomed Mater Res B Appl Biomater. 2011;98B:379–86.
12. Tsang VL, Bhatia SN. Three-dimensional tissue fabrication. Adv Drug Deliver Rev. 2004;56:1635–47.
13. Chen CS, Mrksich M, Huang S, Whitsides GM, Ingber DE. Geometric control of cell life and death. Science. 1997;276:1425–8.
14. Wang PY, Yu J, Lin JH, Tsai WB. Modulation of alignment, elongation and contraction of cardiomyocytes through a

combination of nanotopography and rigidity of substrates. Acta Biomater. 2011. doi:10.1016/j.actbio.2011.05.021.
15. Yeong WY, Sudarmadji N, Yu HY, Chua CK, Leong KF, Venkatraman SS, Boey YCF, Tan LP. Porous polycaprolactone for cardiac tissue engineering fabricated by selective laser sintering. Acta Biomateralia. 2010;6:2028–34.
16. Ciardelli G, Chiono V, Cristallini C, Barbani N, Ahluwalia A, Vozzi G, Previti A, Tantussi G, Giusti P. Innovative tissue engineering structures through advanced manufacturing technologies. J Mater Sci Mater Med. 2004;15:305–10.
17. Rosellini E, Vozzi G, Barbani N, Giusti P, Cristallini C. Three-dimensional microfabricated scaffolds with cardiac extracellular matrix-like architecture. Int J Artif Organs. 2010;33:885–94.
18. Causa F, Netti PA, Ambrosio L. A multi-functional scaffold for tissue regeneration: the need to engineer a tissue analogue. Biomaterials. 2007;28(34):5093–9.
19. Khademhosseini A, Langer R. Nanobiotechnology for drug delivery and tissue engineering. Chem Eng Prog. 2006;102:38–42.
20. Rechichi A, Cristallini C, Vitale U, Ciardelli G, Barbani N, Vozzi G, Giusti P. New biomedical devices with selective peptide recognition properties. Part 1: characterization and cytotoxicity of molecularly imprinted polymers. J Cell Mol Med. 2007;11(6):1367–76.
21. Mosbach K, Ramström O. The emerging technique of molecular imprinting and its future impact on biotechnology. Biotechnology. 1996;14:163–70.
22. Shea KJ. Molecular imprinting of synthetic network polymers: the de novo synthesis of macromolecular binding and catalytic sites. Trends Polym Sci. 1994;2:166–73.
23. Steinke J, Sherrington D, Dunkin I. Imprinting of synthetic polymers using molecular templates. Adv Polym Sci. 1995;123:80–125.
24. Cristallini C, Ciardelli G, Giusti P, Barbani N. Acrylonitrile–acrylic acid copolymer membrane imprinted with uric acid for clinical uses. Macromol Biosci. 2004;4:31–8.
25. Ciardelli G, Borrelli C, Silvestri D, Cristallini C, Barbani N, Giusti P. Supported imprinted nanospheres for the selective recognition of cholesterol. Biosensors Bioelectron. 2006;21:2329–38.
26. Silvestri D, Barbani N, Cristallini C, Giusti P, Ciardelli G. Molecularly imprinted membranes for an improved recognition of biomolecules in aqueous medium. J Membr Sci. 2006;282:284–95.
27. Rosellini E, Barbani N, Giusti P, Ciardelli G, Cristallini C. Novel bioactive scaffolds with fibronectin recognition nanosites based on molecular imprinting technology. J Appl Polym Sci. 2010;118:3236–44.
28. Rosellini E, Barbani N, Giusti P, Rechichi A, Cristallini C. Molecularly imprinted nanoparticles with recognition properties towards a laminin H–Tyr–Ile–Gly–Ser–Arg–OH sequence for tissue engineering applications. Biomed Mater. 2010;5:065007.
29. Cohn D, Younes H. Biodegradable PEO/PLA block copolymers. J Biomed Mater Res. 1988;22:993–1009.
30. Kimura Y, Matsuzaki Y, Yamame H, Kitao T. Preparation of block copoly(ester-ether) comprising poly(l-lactide) and poly(oxypropylene) and degradation of its fibre in vitro and in vivo. Polymer. 1989;30:1342–9.
31. Cerrai P, Tricoli M, Andruzzi F, Paci M, Paci M. Synthesis and characterization of polymers from β-propiolactone and poly(ethylene glycol)s. Polymer. 1987;28:831–6.
32. Cerrai P, Tricoli M, Andruzzi F, Paci M, Paci M. Polyether-polyester block copolymers by non-catalysed polymerization of ε-caprolactone with poly(ethylene glycol). Polymer. 1989;30:338–43.
33. Cerrai P, Tricoli M. Block copolymers from l-lactide and poly(ethylene glycol) through a non-catalyzed route. Makromol Chem Rapid Commun. 1993;14:529–38.
34. Sbarbati-Del Guerra R, Cascone MG, Tricoli M, Cerrai P. In vitro validation of poly(ester–ether–ester) block copolymers as biomaterials. Altern Lab Anim. 1993;21:97–101.
35. Cascone MG, Tricoli M, Cerrai P, Sbarbati Del Guerra R. Cell cultures in the biocompatibility study of synthetic materials. Cytotechnology. 1993;11:S137–9.
36. Cerrai P, Guerra GD, Lelli L, Tricoli M, Sbarbati Del Guerra R, Cascone MG, Giusti P. Poly(ester–ether–ester) block copolymers as biomaterials. J Mater Sci Mater Med. 1994;5:33–9.
37. Cerrai P, Tricoli M, Lelli L, Guerra GD, Sbarbati Del Guerra R, Cascone MG, Giusti P. Block copolymers of L-lactide and poly(ethylene glycol) for biomedical applications. J Mater Sci Mater Med. 1994;5:308–13.
38. Sbarbati Del Guerra R, Cristallini C, Rizzi N, Barsacchi R, Guerra GD, Tricoli M, Cerrai P. The biodegradation of poly(ester–ether–ester) block copolymers in a cellular environment in vitro. J Mater Sci Mater Med. 1994;5:891–5.
39. Sbarbati Del Guerra R, Gazzetti P, Lazzerini G, Cerrai P, Guerra GD, Tricoli M, Cristallini C. Degradation products of poly(ester–ether–ester) block copolymers do not alter endothelial metabolism in vitro. J Mater Sci Mater Med. 1995;6:824–8.
40. Cerrai P, Cristallini C, Del Chicca MG, Guerra GD, Maltinti S, Sbarbati Del Guerra R, Tricoli M. Hydrolysis of poly(ester–ether–ester) block copolymers in the presence of endothelial cells: in vitro modulation of endothelin release. Polym Bull. 1997;39:53–8.
41. Guerra GD, Cristallini C, Barbani N, Gagliardi M. Bioresorbable microspheres as devices for the controlled release of paclitaxel. Int J Biol Biomed Eng. 2011;5:121–8.
42. Wu J, Zeng F, Huang X-P, Chung JC-Y, Konecny F, Weisel RD, Li R-K. Infarct stabilization and cardiac repair with a VEGF-conjugated, injectable hydrogel. Biomaterials. 2011;32:579–86.
43. Vanhoutte D, Schellings M, Pinto Y, Heymans S. Relevance of matrix metalloproteinases and their inhibitors after myocardial infarction: a temporal and spatial window. Cardiovasc Res. 2006;69:604–13.
44. Krumme D, Wenzel H, Tschesche H. Hydroxamate derivatives of substrate-analogous peptides containing aminomalonic acid are potent inhibitors of matrix metalloproteinases. FEBS Lett. 1998;436:209–12.
45. Christman KL, Lee RJ. Biomaterials for the treatment of myocardial infarction. J Am Coll Cardiol. 2006;48:907–13.
46. Chen Q-Z, Harding SE, Ali NN, Lyon AR, Boccaccini AR. Biomaterials in cardiac tissue engineering: ten years of research survey. Mater Sci Eng R. 2008;59:1–37.
47. Nugent HM, Edelman ER. Tissue engineering therapy for cardiovascular disease. Circ Res. 2003;92:1068–78.
48. Agostoni P, Banfi C. Matrix metalloproteinase and heart failure: is it time to move from research to clinical laboratories? Eur Heart J. 2007;28:659–60.
49. Zeugolis, Zeugolis. The physiological relevance of wet versus dry differential scanning calorimetry for biomaterial evaluation. Polym Int. 2010;59:1403–7.
50. Mayes AG, Whitcombe MJ. Synthetic strategies for the generation of molecularly imprinted organic polymers. Adv Drug Delivery Rev. 2005;57:1742–78.
51. Verheyen E, Schillemans JP, van Wijk M, Demeniex M-A, Hennink WE, van Nostrum CF. Challenges for the effective molecular imprinting of proteins. Biomaterials. 2011;32:3008–20.
52. Squire IB, Evans J, Leong LNG, Loftus IM, Thompson MM. Plasma MMP-9 and MMP-2 following acute myocardial infarction in man: correlation with echocardiographic and neurohumoral parameters of left ventricular dysfunction. J Cardiac Fail. 2004;10(4):328–33.